A juvenile mouse pheromone inhibits sexual behavior through the vomeronasal system

Published in final edited form as:
Nature. 2013 October 17; 502(7471): 368–371. doi:10.1038/nature12579.

A juvenile mouse pheromone inhibits sexual behavior through the vomeronasal system

David M. Ferrero[1], **Lisa M. Moeller**[2], **Takuya Osakada**[3], **Nao Horio**[3], **Qian Li**[1], **Dheeraj S. Roy**[1], **Annika Cichy**[2], **Marc Spehr**[2], **Kazushige Touhara**[3,4], and **Stephen D. Liberles**[1,*]

[1]Department of Cell Biology, Harvard Medical School, Boston, MA 02115, USA

[2]Department of Chemosensation, Institute for Biology II, RWTH Aachen University, Aachen, Germany

[3]Department of Applied Biological Chemistry, Graduate School of Agricultural and Life Sciences, The University of Tokyo, Tokyo 113-8657, Japan

[4]ERATO Touhara Chemosensory Signal Project, JST, The University of Tokyo, Tokyo 113-8657, Japan

Animals display a repertoire of different social behaviors. Appropriate behavioral responses depend on sensory input received during social interactions. In mice, social behavior is driven by pheromones, chemical signals that encode information related to age, sex, and physiological state[1]. However, while mice exhibit different social behaviors towards adults, juveniles, and neonates, sensory cues that enable specific recognition of juvenile mice are unknown. Here, we describe a juvenile pheromone produced by young mice before puberty, termed exocrine-gland secreting peptide 22 (ESP22). ESP22 is secreted from the lacrimal gland and released into tears of 2–3 week old mice. Upon detection, ESP22 activates high affinity sensory neurons in the vomeronasal organ (VNO), and downstream limbic neurons in the medial amygdala. Recombinant ESP22, painted on mice, exerts a powerful inhibitory effect on adult male mating behavior, and this effect is abolished in knockout mice lacking TRPC2, a key signaling component of the VNO[2,3]. Furthermore, knockout of TRPC2 or loss of ESP22 production results in increased sexual behavior of adult males towards juveniles, and sexual responses towards ESP22-deficient juveniles are suppressed by ESP22 painting. Thus, we describe a pheromone of sexually immature mice that controls an innate social behavior, a response pathway through the accessory olfactory system, and a novel role for VNO signaling in inhibiting sexual behavior towards young. These findings provide a molecular framework for understanding how a sensory system can regulate behavior.

We developed a genome-based strategy for identification of additional mouse pheromones (Fig 1a). Chemicals that function as pheromones include urinary volatiles, steroid derivatives, and proteins secreted into bodily fluids such as urine, tears, and saliva[4–7]. Several protein pheromones are encoded by large, rapidly evolving gene families, but the vast majority of pheromone homologs encoded by the mouse genome are of unknown function[8–10]. We constructed qPCR primers to detect expression of protein pheromones and

*Corresponding Author: Stephen_Liberles@hms.harvard.edu, phone: (617) 432-7283, fax: (617) 432-7285.

Supplementary Information is available in the online version of the paper.

Author Contributions

D.M.F., S.D.L., M.S., and K.T. conceived the project, designed the experiments, and wrote the manuscript. D.M.F. performed molecular biology, biochemistry, and behavior experiments. D.S.R. and Q.L. performed *in situ* hybridization analysis. L.M.M., A.C., T.O., and N.H. performed electrophysiological analysis. T.O. performed cFos analysis.

The authors declare no competing financial interests.

their homologs, including exocrine gland-secreting peptides (ESPs), androgen binding proteins (ABPs), major urinary proteins (MUPs), and other lipocalins. Expression levels were quantified in cDNA derived from various pheromone-producing tissues obtained from mice of different sexes, ages, and physiological states.

Using this strategy, we identified several peptides with striking age-dependent production in the extraorbital lacrimal gland (LG), including ESP22 produced by juveniles, ESP15 and ESP16 produced by adults of both sexes, and ABP27 produced by neonates (Fig. 1b, Extended Data Fig. 1a). We also identified male-enriched peptides of unknown function, including ESP24 and various ABPs. Interestingly, sexually dimorphic production of ESP24 and the male pheromone ESP1 was similar (~500-fold male-enriched), but occurred in different mouse strains (Extended Data Fig. 2b).

Since juvenile pheromones are unknown, we performed additional studies of ESP22. ESP22 was maximally expressed in LG between 2–3 weeks of age, and decreased sharply after 4 weeks of age, near puberty (Fig. 1b). Quantitative analysis indicated ESP22 expression in LG to be similar in male and female juveniles, and ~50-fold higher in juveniles than adults (Extended Data Fig. 2d). ESP22 expression was not detected in cDNA derived from 16 other mouse tissues, including other exocrine glands, internal organs, and sensory epithelia (Fig. 1c, Extended Data Fig. 2f). In contrast, ABP27 expression was detected in adult salivary gland as well as neonatal LG (Extended Data Fig. 2e).

Next, we identified LG cell types that expressed ESP22 and other pheromone homologs using RNA *in situ* hybridization (ISH). We found that ESP22 is produced by a subset of lacrimal secretory cells, termed acinar cells (Extended Data Fig. 1c), which release contents into tears, a source of mouse pheromones[9]. ESP22 expression was detected in juvenile but not adult acinar cells, while ESP24 expression was detected only in adult male acinar cells (Fig. 1d). Furthermore, *Esp22* was not expressed in castrated and ovariectomized adults, suggesting sex hormone-independent *Esp22* gene regulation (Extended Data Fig. 1b).

To test whether ESP22 protein was secreted into tears by acinar cells, we generated and affinity-purified a polyclonal anti-ESP22 antibody. Western Blot analysis using this antibody identified a ~10 kD protein of expected mass that was enriched in juvenile tears (Fig. 1e). Levels of this protein (3–5 ng/μl in juvenile tears, or ~300–500 nM) were determined using a standard curve of recombinant ESP22 (Extended Data Fig. 3). Mass spectrometry (MS) identified ESP22-derived tryptic peptides in tears of juveniles but not adults, indicating >100-fold enrichment (Fig. 1f), and revealed the primary structure of mature ESP22 (amino acids 23–111, Extended Data Fig. 4). Together, these findings indicate that ESP22 is a lacrimal peptide secreted into tears of juvenile mice.

Next, we asked whether ESP22 was detected by the mouse olfactory system. Other protein pheromones, including ESP1, activate basal VNO sensory neurons[11], so we examined electrophysiological responses to ESP22 in the VNO. Recombinant ESP22 was prepared as a fusion protein with maltose binding protein (MBP), which enhanced solubility[12]. Electrovomeronasogram (EVG) recordings indicated that recombinant ESP22 (200 nM) evoked a negative field potential in the VNO (Fig. 2a), with sensitivity matching ESP1 responses previously reported with this technique[13,14]. MBP was not similarly detected, although small EVG responses to MBP were observed at higher concentrations (data not shown). High affinity responses to ESP22 in the VNO required the ion channel TRPC2 (Fig. 2a), and were not observed in electroolfactogram (EOG) recordings of the main olfactory epithelium (Fig. 2b), which is also important for pheromone-driven social behaviors[15–17].

Next, we used extracellular loose-seal recordings to examine ESP22 responses in individual VNO sensory neurons. ESP22 evoked robust and repetitive discharge patterns in 1.3% of

basal VNO sensory neurons (5/383), consistent with detection by one or a few VNO receptors (Fig. 2c, Extended Data Fig. 5 for higher [ESP22]). Threshold ESP22 responses observed by single unit extracellular recordings (Fig. 2d) occurred at similar concentrations (20 pM) to threshold ESP1 responses previously measured using genetically encoded calcium indicators[18]. The majority of neurons responsive to ESP22 were activated by juvenile tears but not by MBP or adult tears (6/11, Fig. 2e, Extended Data Fig. 5), with neuron viability verified by K^+-mediated depolarization. High affinity ESP22 responses were also recorded in ~1–2% of VNO sensory neurons using current clamp recording techniques and single neuron calcium imaging (data not shown).

We next identified limbic neurons activated by ESP22 exposure using immunohistochemistry (IHC) for the neural activity marker cFos in cryosections of adult male mouse brains. ESP22 and juvenile tears (Fig. 2f, Extended Data Fig. 6) induced cFos expression in the medial amygdala (MeA), a region that receives VNO input by way of the accessory olfactory bulb[13,19]. cFos responses were not observed in *Trpc2*$^{-/-}$ mice (Fig. 2f), or in other amygdala regions that receive olfactory input (Extended Data Fig. 6). cFos responses were enriched in the postero-ventral MeA (Fig. 2g), which sends projections to hypothalamic areas that control defensive and reproductive responses[20,21].

These findings indicate ESP22 to be a juvenile chemosignal that activates a VNO response pathway. However, a role for the VNO in regulating adult-juvenile social interactions is unknown. *Trpc2*$^{-/-}$ mice provide a valuable tool for VNO loss-of-function studies, and display severe deficits in sex recognition[2,3]. Here, we introduced *Trpc2*$^{+/+}$ or *Trpc2*$^{-/-}$ males to juveniles and monitored social behavior.

Surprisingly, we observed that *Trpc2*$^{-/-}$ mice displayed a striking increase in sexual behavior towards prepubescent females (Supplementary Videos 1, 2). While *Trpc2*$^{+/+}$ mice displayed rare mounting attempts towards juvenile females, *Trpc2*$^{-/-}$ mice displayed vigorous mounting behavior quantified as increases in mean mounting attempts and percentage of animals mounting within 3 and 10 minutes, as well as decreases in mounting latency and intermount interval (Fig. 3, Extended Data Fig. 7a). A similar percentage of *Trpc2*$^{+/+}$ males displayed mounting behavior by 30 minutes, but these mounts were rare and did not increase in frequency during the trial duration (Fig. 3d, Extended Data Fig. 7b). In contrast, the sexual behavior of *Trpc2*$^{-/-}$ and *Trpc2*$^{+/+}$ males towards adult females was similar, as reported previously[2,3]. *Trpc2*$^{-/-}$ mice displayed sexual behavior towards juvenile females even when presented simultaneously with adult estrous females (Extended Data Fig. 7c), and also exhibited increased sexual behavior towards juvenile males (Extended Data Fig. 8). Based on these findings, VNO signaling normally prevents mating advances towards young, and one mechanism likely involves detection of chemosignals released from juvenile animals.

We reasoned that ESP22 is an excellent candidate to function as such a mating inhibitor based on the timing of its expression, the role of another ESP as a pheromone[13], and the ability of ESP22 to activate both VNO sensory neurons and central limbic regions. ESP22 is juvenile-enriched in several strains of mice, but we identified two strains (C3H and CBA) that lacked juvenile ESP22 expression (Fig 4a). These mouse strains provided valuable tools for controlling ESP22 levels during social interactions, and we observed increased sexual behavior of wild type males towards C3H and CBA juveniles (Fig. 4b).

We asked whether painting recombinant ESP22 onto C3H juveniles blocked male sexual approaches. We observed that males displayed similar levels of sexual behavior towards unpainted, ESP6-painted, and MBP-painted C3H juveniles (Fig. 4d). However, males displayed a significant reduction in mounting attempts and an increase in mounting latency

towards C3H juveniles painted with ESP22 (1 ng). Higher ESP22 levels (10 μg) caused a striking 70-fold reduction in mounting attempts towards C3H juveniles, with most animals (10/11) failing to display a single mating attempt during the entire 30 minute trial (Fig. 4c, 4d). A dose-dependent analysis indicated that amounts of ESP22 derived from small quantities of juvenile tears (< 200–333 nl) were sufficient for inhibition of adult male sexual behavior (Fig. 4e). ESP22 was not aversive, as ESP22 painting did not impact social interaction time (Extended Data Fig. 9). ESP22 also did not inhibit sexual behavior of *Trpc2*$^{-/-}$ males, consistent with a role for vomeronasal circuits in mediating ESP22 responses (Fig. 4f). Interestingly, *Trpc2*$^{-/-}$ males did not display further increases in sexual behavior towards C3H juveniles (Fig. 4f), suggesting that C3H juveniles do not release other VNO-dependent mating inhibitors. However, ESP22 did inhibit the sexual behavior of C3H adult males, who presumably have encountered little or no ESP22 previously (Extended Data Fig. 10). Finally, recombinant ESP22 also decreased sexual behavior towards adult females in estrous (Fig. 4g). Lower levels of sexual behavior persisted towards ESP22-painted estrous females, suggesting that estrous females release other signals that counteract ESP22. Based on these findings, ESP22 is a juvenile pheromone that blocks sexual behavior through the vomeronasal system (Fig. 4h).

Behavioral responses to ESP22 differ from responses to other VNO activators, such as pheromones and predator odors that trigger mating, aggression, and fear[12,13,22,23]. These findings are consistent with the existence of parallel subcircuits of the accessory olfactory system which selectively channel sensory inputs to enable proper selection of a behavioral display[20]. Identifying a collection of VNO activators that regulate different instinctive behaviors provides a valuable toolbox to understand how a sensory system controls behavior.

Methods

Animals

All animal procedures were in compliance with institutional animal care and use committee guidelines. Mice from various strains, as well as castrated and ovariectomized animals, were obtained from Jackson Laboratory (Bar Harbor, ME) and Charles River Laboratories (Wilmington, MA) unless otherwise noted. *Trpc2*$^{-/-}$ mice were generously provided by Richard Axel (Columbia University). C3H mice refer to the strain C3H/He. Estrous was induced in ovariectomized adult females (C57BL/6, 10–12 weeks) by timed injection of estradiol benzoate (Sigma-Aldrich, 10 μg sesame seed oil, subcutaneous injection) 48 h and 24 h before testing, and progesterone (Sigma-Aldrich, 500 μg in sesame seed oil, subcutaneous injection) 3 h before testing.

qPCR analysis

cDNAs from the extraorbital lacrimal gland and other tissues were prepared from animals of ages and sexes indicated using published protocols[28]. Copy number, unless otherwise indicated, refers to abundance in cDNA derived from 50 ng of RNA, with absolute values determined in control PCR reactions involving plasmid titrations. qPCR primers were verified not to cross react with closely related ESPs and ABPs (>60% identity) based on control reactions involving ESP- and ABP-encoding plasmids (Extended Data Fig. 2a). (*Esp22* forward: 5'-GTCCCGGAATCTGTTATCCA-3'; *Esp22* reverse: 5'-CAGCAATGCTCACTGAAGGA-3'. *Esp15* forward: 5'-AACAGGAGCTGCTCTGAATTA-3'; *Esp15* reverse: 5'-GCCTATGACAGAGCCACTTA-3'. *Esp16* forward: 5'-TCTGTGTCTCATGCACTGCTTCCT-3'; *Esp16* reverse: 5'-GGAAGTATTGTTGGAAACACCAGAAA-3'. *Esp6* forward: 5'-

TCCTTGGTCCTGAGATTGCT-3'; *Esp6* reverse: 5'-TTTGCTCACCAACCCAACCA-3'. β*27* forward: 5'-GGTGGAAATAGGCTAGCTCTGA-3'; β*27* reverse: 5'-GGGTTCCAGAAGTATATTTCTTATA-3'. β*2* forward: 5'-AGCATGCATACCTTTCTTCGGCGTA-3'; β*2* reverse: 5'-TGCATTCTGAGCTGAAGAGTATAGTTGT-3'.) Different primers were used in PCR reactions described in Fig. 1c (*Esp22* forward: 5'-ATGAATTCTGTCCCAGTCATG-3'; *Esp22* reverse: 5'-TCAAGTATTTGTCAAAAGGCGT-3'), and specific amplification of the *Esp22* gene was verified by DNA sequencing.

RNA *in situ* hybridization

In situ hybridization analysis of lacrimal gland tissue was performed using established techniques involving colorimetric visualization[29] or multicolor fluorescence[30]. cRNA riboprobes were used for *Esp22* (full coding sequence plus 500 base pairs of the 3' untranslated region), *Esp24* and *Esp15* (full coding sequence), and *Rab3D* (926 base pair sequence amplified by primers TTCCGCTATGCCGATGACTC and TGACAACTTCAGCCAGCGAT). The *Esp22* riboprobe shares <75% identity with other *Esp* genes, a level of identity below what typically results in cross-hybridization under high stringency conditions used. Furthermore, *Esp22* is most closely related to *Esp24*, and we did not observe cross-hybridization between these genes (Fig. 1d). Images were taken on a Nikon 80i upright microscope for colorimetric images, and on a Leica TCS SP5 II confocal microscope for fluorescent images.

Western Blot analysis

Anesthetized mice were injected with pilocarpine (Sigma-Aldrich, 0.5 μg/g body weight, i.p.) and tear fluid was collected using microcapillary pipets. Proteins in tear fluid were separated by electrophoresis using 16.5% Tris-tricine gels (Biorad), transferred to PVDF membranes (Immobulin), and incubated with a rabbit polyclonal antibody raised against ESP22 (amino acids 51–63: CRRLRDVPESVIH, New England Peptide, 1:500, 24–48 h, 4°C). Bound antibody was detected with a donkey anti-rabbit 800 Infrared Dye (Odyssey, 5000:1, 45 min, RT). Blots were analyzed using a Quantitative IR Western Blot Detection LI-COR (Odyssey) and the Li-COR Quantitative Gel Documentation and Blot Detection Software (Odyssey).

Mass spectrometry

Tear fluid was collected and separated by gel electrophoresis as described above. Excised gel bands containing ~3–14 kD proteins were then subjected to a modified in-gel trypsin digestion procedure[31]. Samples were loaded via a Famos auto sampler (LC Packings) onto a nano-scale reverse-phase HPLC capillary column[32], and eluted using a gradient of increasing acetonitrile containing 0.1% formic acid. Eluted peptides were subjected to electrospray ionization and analyzed by an LTQ-Orbitrap mass spectrometer (Thermo Fisher). Eluted peptides were isolated, including those corresponding to m/z 612.4 and 446.3 (the +2 charges states of the ESP22 tryptic peptides DVPESVIHISK and GIVFNTIK), and fragmented to produce a tandem mass spectrum of specific fragment ions for each peptide. Peptide sequences were determined using Sequest (ThermoFinnigan)[33].

Recombinant proteins

A gene encoding the secreted form of ESP22 (Ala23-End) was cloned into **pMAL-c5x** bacterial expression vector (New England Biolabs) using SacI and BamHI restriction sites. ESP22 was expressed and purified as a fusion protein with maltose-binding protein (MBP) in BL21(DE3) cells following manufacturer's protocols (pMAL Protein Fusion & Purification System, New England Biolabs). Protein was eluted from an amylose affinity

resin using maltose and concentrated using a centrifugal filter unit (Millipore). The ESP6 coding sequence was subcloned into the expression vector pET-28a (Novagen) and purified as described previously[17].

Electrophysiology

EVG, EOG, and extracellular recordings were performed as described previously with minor modifications[17,34,35]. To prevent dialysis of intracellular components, action potential-driven capacitive currents were recorded in 'loose-seal' cell-attached configuration (seal resistance 30 – 150 MΩ) from VSN somata located deep in the sensory epithelium's basal layer close to the basement membrane. Spikes were analyzed using Igor Pro functions (SpAcAn, G. Dugué and C. Rousseau). Inter-stimulus intervals were 30 s. Neuronal responses were classified according the following criteria: a) discharge was time-locked to stimulus presentation (responses occurred during and/or up to 3 s after stimulation onset); b) spike patterns clearly deviated from prior baseline activity (frequency histograms (1 s bin width) were calculated over repeated trials and responses were evaluated according to a $\Delta f \geq 2 \times \mathrm{SD}\ f_{(\mathrm{baseline})}$ criterion). MBP and ESP22 evoked TRPC2-independent EVG and EOG responses at ~100-fold higher concentrations (data not shown).

cFos staining

Sexually naive males (Japan SLC, C57BL/6, 9–11 weeks old) were housed individually (17×25 cm Plexiglas test chambers, 12 h light/12 h dark cycle). Stimuli included ESP22 (250 μg), tear fluid (containing 50 μg protein), or MBP (200 μg) in 20 mM Tris-HCl (pH 7.5, 100 μl) transfused onto a piece of cotton (30 mg) and dried in a Speed Vac (3 hours). High concentrations of ESP22 were necessarily used for cFos studies, as this non-volatile stimulus is poorly investigated when presented in isolation. Stimuli were placed on bedding during the dark phase (90 minutes), and all mice were observed to investigate the stimulus during testing. Mice were then anaesthetized with pentobarbital sodium and perfused quickly. Brains were removed and post-fixed in 4% paraformaldehyde in PBS (3 h, 4°C) and cryoprotected in 15% and 30% sucrose solutions in PBS (4°C). IHC and quantification of cFos-positive nuclei were performed as described previously[16]. MeA regions were defined using established anatomical landmarks (Extended Data Fig. 6), comparison with a reference image (Bregma −1.58 mm)[36], and Lhx9 staining[23] (data not shown).

Behavior

Prior to experiments, sexually naive adult males (2–4 months old, C57BL/6 *Trpc2*$^{+/+}$ or *Trpc2*$^{-/-}$) were maintained under a reverse light cycle for 2 weeks and individually housed for ≥ 24 hours. Behavioral testing occurred in the home cage with the food tray removed > 3 hours after onset of dark phase. A sexually naive male or female (17–18 day old juvenile or adult in estrous) was introduced with the male, and interaction behavior was recorded for 30 minutes using a digital camcorder compatible with low light conditions (Sony). For some experiments, females were painted by swabbing stimulus (100 μl) on the back (50 μl), head (25 μl), and anogenital region (25 μl) prior to testing. Mounting behavior was defined when males used both forepaws to climb onto a female for copulation, and parameters associated with mounting behavior were analyzed using Matlab (Mathworks). In rare cases (< 5%), juvenile pups displayed stimulus-independent escape behavior and were excluded from analysis. Animals were randomly assigned to different testing conditions. For Figure 4 (c–e), quantification was performed blind to experimental conditions.

Statistical analyses

All samples represent biological replicates. Sample sizes for biochemistry, electrophysiology, cFos, and behavior meet or exceed the standards in the field. In Figure

1b, sample sizes (n) for data points reading left to right are 12, 7, 7, 8, 6, 13 for *Esp22*; 12, 7, 8, 8, 6, 12 for *Esp6*; 8, 5, 5, 7, 6, 12 for *Esp15*; 8, 8, 10, 8, 4, 8 for *Abp-β27*; 11, 8, 10, 8, 6, 10 for *Abp-β2*; and 8, 5, 6, 6, 5, 10 for *Esp16*. In Figure 4a, sample sizes reading left to right are 13, 10, 6, 6, 5, 7, 5, and 7. In Figure 4b, sample sizes reading left to right are 12, 9, 9, and 14. In Figure 4d, sample sizes reading left to right are 14, 12, 11, and 9. In Figure 4e, sample sizes reading left to right are 14, 12, 12, 12, 11, 11, and 11. In Figure 4f, samples sizes reading left to right are 12, 12, and 11. In Figure 4g, sample sizes reading left to right are 12, 11, and 11. Categorical data was analyzed by a Fisher's exact test. Other reported p values were calculated using one-tailed Student's t-test (qPCR, cFos), Mann-Whitney *U* tests (mouse behavior), or one- or two-way ANOVA followed by Tukey's HSD (honestly significant difference) post hoc tests (mouse behavior), as indicated in the figure legends.

Supplementary Material

Refer to Web version on PubMed Central for supplementary material.

Acknowledgments

We thank Mark Albers and Sandeep Robert Datta for careful reading of the manuscript, Jenny Yang, C. Mark Fletcher, and Yaw Tachie-Baffour for experimental assistance, and the Taplin Mass Spectrometry Facility for MS analysis. This work was supported by a grant from the NIH (SDL, Award Number R01 DC010155) and in part by a Grant-in-Aid for Young Scientists (S) from JSPS, and by ERATO Touhara Chemosensory Signal Project from JST (to KT). NH is supported by a Grant-in-Aid for JSPS Fellows, MS is a Lichtenberg-Professor of the Volkswagen Foundation, and DMF is supported by a Boehringer Ingelheim Fonds PhD Fellowship.

References

1. Tirindelli R, Dibattista M, Pifferi S, Menini A. From pheromones to behavior. Physiological reviews. 2009; 89:921–956. [PubMed: 19584317]
2. Leypold BG, et al. Altered sexual and social behaviors in trp2 mutant mice. Proceedings of the National Academy of Sciences of the United States of America. 2002; 99:6376–6381. [PubMed: 11972034]
3. Stowers L, Holy TE, Meister M, Dulac C, Koentges G. Loss of sex discrimination and male-male aggression in mice deficient for TRP2. Science (New York, N.Y. 2002; 295:1493–1500.
4. Ferrero DM, Liberles SD. The secret codes of mammalian scents. Wiley Interdiscip Rev Syst Biol Med. 2010; 2:23–33. [PubMed: 20836008]
5. Nodari F, et al. Sulfated steroids as natural ligands of mouse pheromone-sensing neurons. J Neurosci. 2008; 28:6407–6418. [PubMed: 18562612]
6. Novotny MV. Pheromones, binding proteins and receptor responses in rodents. Biochemical Society transactions. 2003; 31:117–122. [PubMed: 12546667]
7. Touhara K. Sexual communication via peptide and protein pheromones. Curr Opin Pharmacol. 2008; 8:759–764. [PubMed: 18824132]
8. Karn RC, Laukaitis CM. The roles of gene duplication, gene conversion and positive selection in rodent esp and mup pheromone gene families with comparison to the abp family. PLoS One. 2012; 7:e47697. [PubMed: 23094077]
9. Kimoto H, Haga S, Sato K, Touhara K. Sex-specific peptides from exocrine glands stimulate mouse vomeronasal sensory neurons. Nature. 2005; 437:898–901. [PubMed: 16208374]
10. Logan DW, Marton TF, Stowers L. Species specificity in major urinary proteins by parallel evolution. PLoS One. 2008; 3:e3280. [PubMed: 18815613]
11. Chamero P, et al. G protein G(alpha)o is essential for vomeronasal function and aggressive behavior in mice. Proceedings of the National Academy of Sciences of the United States of America. 2011; 108:12898–12903. [PubMed: 21768373]
12. Papes F, Logan DW, Stowers L. The vomeronasal organ mediates interspecies defensive behaviors through detection of protein pheromone homologs. Cell. 2010; 141:692–703. [PubMed: 20478258]

13. Haga S, et al. The male mouse pheromone ESP1 enhances female sexual receptive behaviour through a specific vomeronasal receptor. Nature. 2010; 466:118–122. [PubMed: 20596023]
14. Kimoto H, et al. Sex- and strain-specific expression and vomeronasal activity of mouse ESP family peptides. Curr Biol. 2007; 17:1879–1884. [PubMed: 17935991]
15. Li Q, et al. Synchronous evolution of an odor biosynthesis pathway and behavioral response. Curr Biol. 2013; 23:11–20. [PubMed: 23177478]
16. Mandiyan VS, Coats JK, Shah NM. Deficits in sexual and aggressive behaviors in Cnga2 mutant mice. Nature neuroscience. 2005; 8:1660–1662.
17. Wang Z, et al. Pheromone detection in male mice depends on signaling through the type 3 adenylyl cyclase in the main olfactory epithelium. J Neurosci. 2006; 26:7375–7379. [PubMed: 16837584]
18. He J, et al. Distinct signals conveyed by pheromone concentrations to the mouse vomeronasal organ. J Neurosci. 2010; 30:7473–7483. [PubMed: 20519522]
19. Dulac C, Wagner S. Genetic analysis of brain circuits underlying pheromone signaling. Annu Rev Genet. 2006; 40:449–467. [PubMed: 16953793]
20. Choi GB, et al. Lhx6 delineates a pathway mediating innate reproductive behaviors from the amygdala to the hypothalamus. Neuron. 2005; 46:647–660. [PubMed: 15944132]
21. Yang CF, et al. Sexually dimorphic neurons in the ventromedial hypothalamus govern mating in both sexes and aggression in males. Cell. 2013; 153:896–909. [PubMed: 23663785]
22. Chamero P, et al. Identification of protein pheromones that promote aggressive behaviour. Nature. 2007; 450:899–902. [PubMed: 18064011]
23. Novotny M, Harvey S, Jemiolo B, Alberts J. Synthetic pheromones that promote inter-male aggression in mice. Proceedings of the National Academy of Sciences of the United States of America. 1985; 82:2059–2061. [PubMed: 3856883]

References

28. Liberles SD, Buck LB. A second class of chemosensory receptors in the olfactory epithelium. Nature. 2006; 442:645–650. [PubMed: 16878137]
29. Montmayeur JP, Liberles SD, Matsunami H, Buck LB. A candidate taste receptor gene near a sweet taste locus. Nat Neurosci. 2001; 4:492–498. [PubMed: 11319557]
30. Liberles SD, et al. Formyl peptide receptors are candidate chemosensory receptors in the vomeronasal organ. Proceedings of the National Academy of Sciences of the United States of America. 2009; 106:9842–9847. [PubMed: 19497865]
31. Shevchenko A, Wilm M, Vorm O, Mann M. Mass spectrometric sequencing of proteins silver-stained polyacrylamide gels. Anal Chem. 1996; 68:850–858. [PubMed: 8779443]
32. Peng J, Gygi SP. Proteomics: the move to mixtures. Journal of mass spectrometry : JMS. 2001; 36:1083–1091. [PubMed: 11747101]
33. Eng JK, Mccormack AL, Yates JR. An Approach to Correlate Tandem Mass-Spectral Data of Peptides with Amino-Acid-Sequences in a Protein Database. J Am Soc Mass Spectr. 1994; 5:976–989.
34. Hagendorf S, Fluegge D, Engelhardt C, Spehr M. Homeostatic control of sensory output in basal vomeronasal neurons: activity-dependent expression of ether-a-go-go-related gene potassium channels. J Neurosci. 2009; 29:206–221. [PubMed: 19129398]
35. Spehr J, et al. Ca2+-calmodulin feedback mediates sensory adaptation and inhibits pheromone-sensitive ion channels in the vomeronasal organ. J Neurosci. 2009; 29:2125–2135. [PubMed: 19228965]
36. Franklin, K.; Paxinos, G. The mouse brain in stereotaxic coordinates. Academic Pres; 2008.

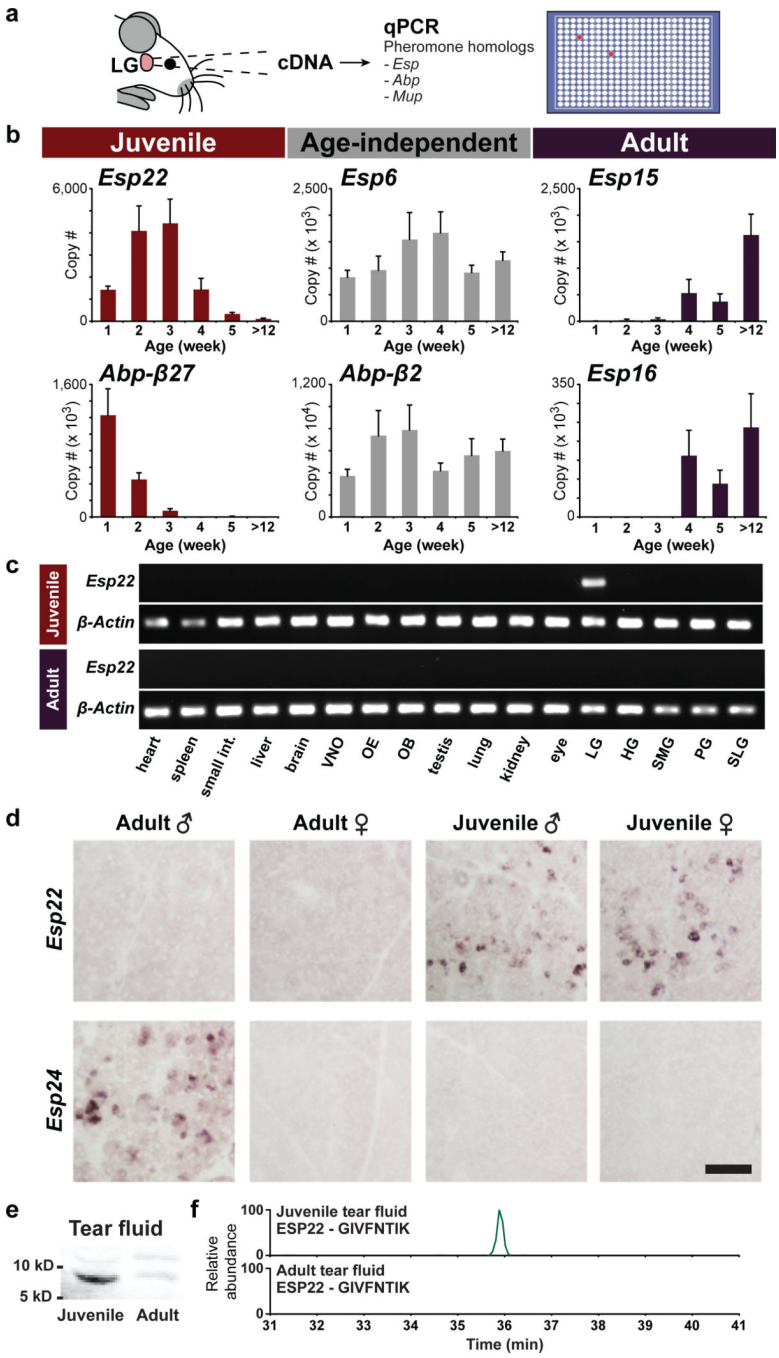

Figure 1. ESP22 is secreted into juvenile tear fluid

a, Strategy to identify mouse pheromones. **b**, Age-dependent gene expression in lacrimal gland (LG) determined by qPCR (n=4–12, mean, ± s.e.m.). **c**, *Esp22* expression in juvenile and adult tissues determined by RT-PCR; olfactory epithelium (OE), olfactory bulb (OB), harderian gland (HG), submaxillary gland (SMG), parotid gland (PG), sublingual gland (SLG). **d**, Age- and sex-dependent *Esp* expression in LG determined by *in situ* hybridization. Scale bar, 100 μm. **e**, Western blot analysis of tears using anti-ESP22 antibody. **f**, MS analysis of an ESP22-derived tryptic peptide (GIVFNTIK) from tears.

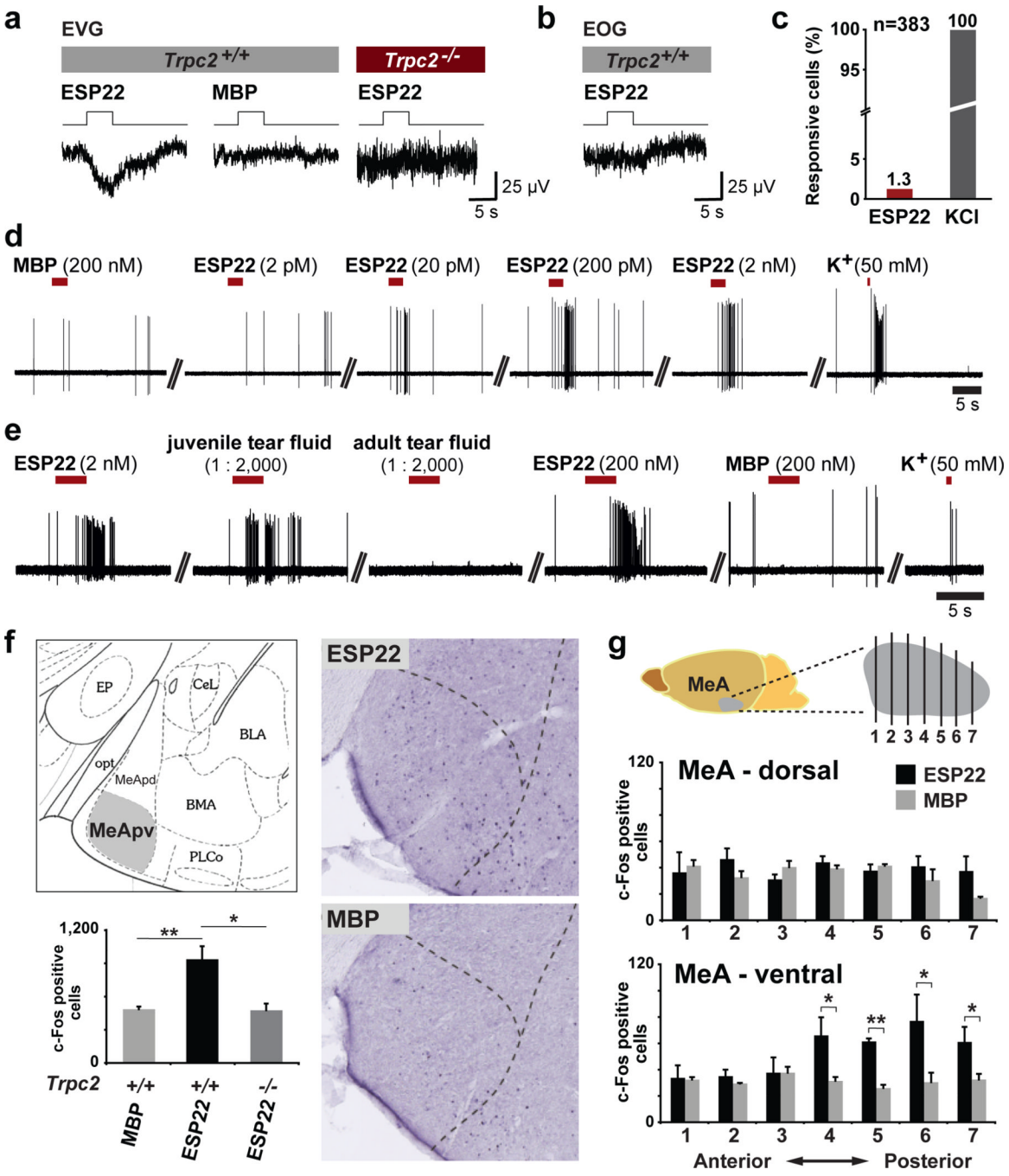

Figure 2. ESP22 activates the vomeronasal system

a, EVG and **b**, EOG recordings in *Trpc2*$^{-/-}$ and *Trpc2*$^{+/+}$ mice exposed to ESP22 (200 nM) and MBP (450 nM) **c**, The percentage of basal VNO sensory neurons (n=383) responsive to ESP22 (20 pM) and KCl (50 mM) determined by single-unit extracellular loose-seal recordings. **d–e**, Responses of single VNO sensory neurons. **f–g**, Visualization and quantification of cFos-expressing neurons in MeA, determined by IHC in coronal brain sections from ESP22- and MBP-exposed male mice. (mean ± s.e.m., n=3, *p<0.05, **p<0.01, Student's one-tailed t test).

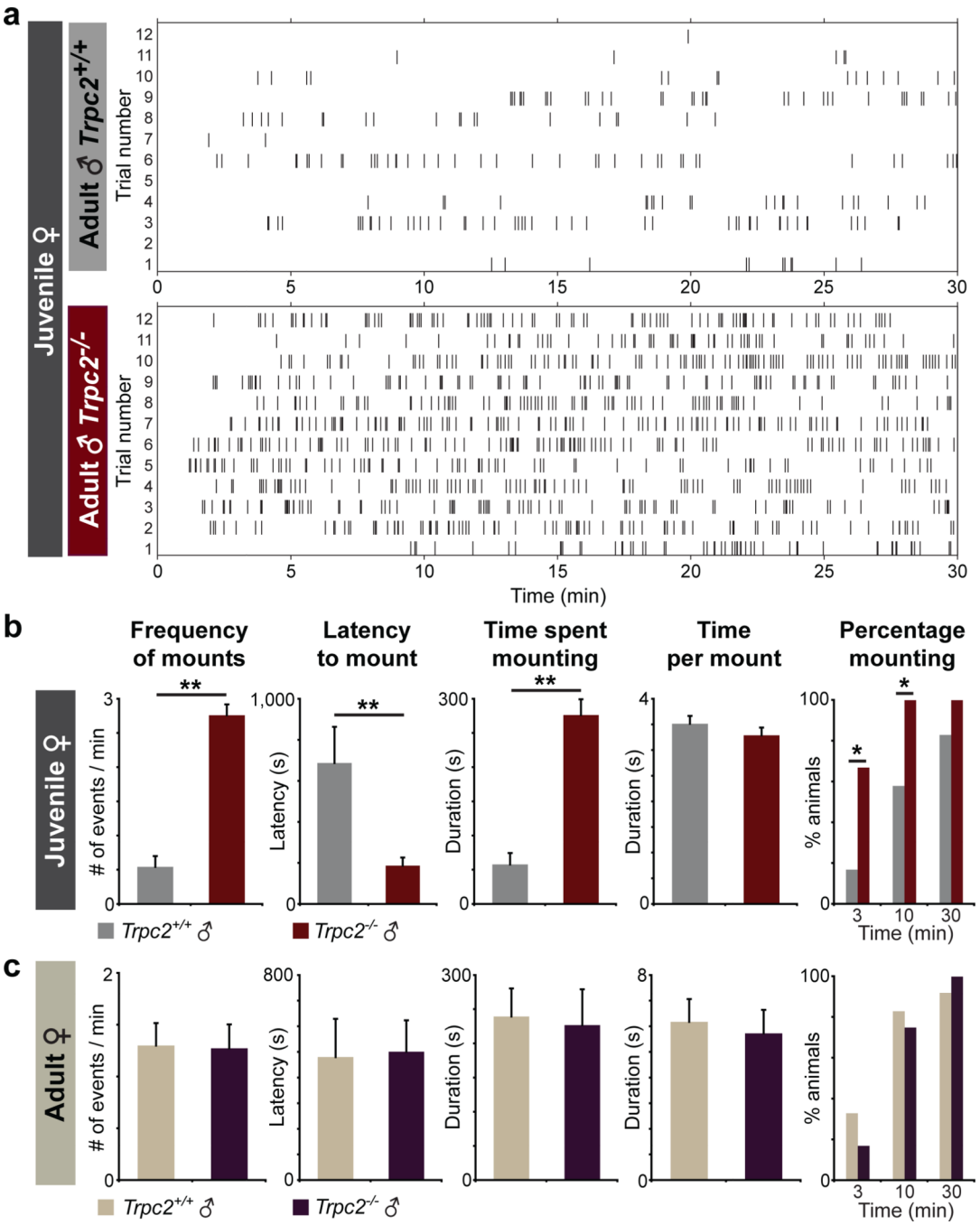

Figure 3. *Trpc2*$^{-/-}$ males display increased sexual behavior towards juveniles

a, Raster plots depicting individual mounting displays of adult *Trpc2*$^{+/+}$ and *Trpc2*$^{-/-}$ males (n=12) towards female juveniles (C57BL/6, 2–3 weeks old) during behavioral testing (30 min). Each tick indicates onset of one mount. **b–c**, Quantitative analysis of parameters associated with sexual behavior towards juvenile and adult females displayed by *Trpc2*$^{+/+}$ and *Trpc2*$^{-/-}$ males. (mean ± s.e.m., *p<0.05, **p<0.01, Mann-Whitney *U* test).

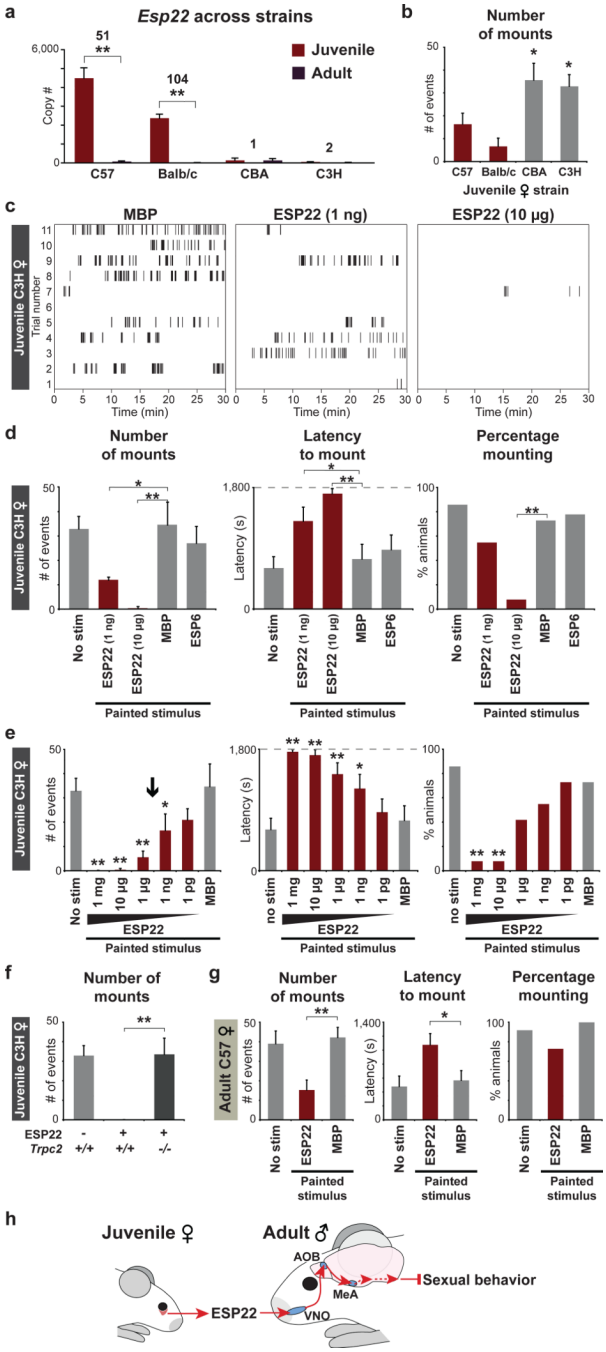

Figure 4. ESP22 inhibits male sexual behavior

a, ESP22 levels in LG from mouse strains and ages indicated (n=5–12, averages ± s.e.m.). **b**, Sexual behavior of wild type males towards juveniles from strains indicated (n=11–12). **c–g**, Raster plots and quantification of sexual behavior displayed by wild type males (**d–f**) or *Trpc2*$^{-/-}$ males (**f**) towards C3H juveniles (**d–f**) or C57BL/6 estrous females (**g**) painted with ESP6 (10 µg), ESP22 (10 µg or indicated), or MBP (4 mg) (n=9–12, averages ± s.e.m.). Arrow depicts ESP22 concentration in C57BL/6 juvenile tears. **h**, Model for ESP22 signaling. *p<0.05, **p<0.01, Student's one-tailed t test (**a**), one-way (**b**, **d**, **e**, **g**) or two-way (**f**) ANOVA followed by Tukey's HSD post hoc tests.